Coupon position does not affect Pseudomonas aeruginosa and Staphylococcus aureus biofilm densities in the CDC biofilm reactor

Elizabeth Buckner, Kelli Buckingham-Meyer, Lindsey A. Miller, Albert E. Parker, Christopher J. Jones, Darla M. Goeres

Coupon Position Does Not Affect *Pseudomonas aeruginosa* and *Staphylococcus aureus* Biofilm Densities in the CDC Biofilm Reactor

Center for Biofilm Engineering

Montana State University

366 Barnard Hall

P.O. Box 173980

Bozeman, MT 59717-3980

Elizabeth Buckner: elizabethmb31@gmail.com

Kelli Buckingham-Meyer: kellib@montana.edu

Lindsey Miller: lindsey.lorenz@montana.edu

Albert E. Parker: albert.parker@montana.edu

Christopher Jones: christopher.jones23@montana.edu

Darla M. Goeres: darla_g@montana.edu: Corresponding author

Abstract

The CDC Biofilm Reactor method is the standard biofilm growth protocol for the validation of US Environmental Protection Agency biofilm label claims. However, no studies have determined the effect of coupon orientation within the reactor on biofilm growth. If positional effects have a statistically significant impact on biofilm density, they should be accounted for in the experimental design. Here, we isolate and quantify biofilms from each possible coupon surface in the reactor to quantitatively determine the positional effects in the CDC Biofilm Reactor. The results showed no statistically significant differences in viable cell density across different orientations and vertical positions in the reactor. *Pseudomonas aeruginosa* log densities were statistically equivalent among all coupon heights and orientations. While the *Staphylococcus aureus* cell growth showed no statistically significant differences, the densities were not statistically equivalent among all coupon heights and orientations due to the variability in the data. Structural differences were observed between biofilms on the high-shear baffle side of the reactor compared to the lower shear glass side of the reactor. Further studies are required to determine whether biofilm susceptibility to antimicrobials differs based on structural differences attributed to orientation.

Keywords

CDC reactor, coupon, equivalence, height, orientation

Introduction

Biofilms are self-organized, cooperative communities of bacteria embedded in an extracellular matrix and are known to impact multiple industries. Biofilm is associated with chronic infections (Bjarnsholt, 2013), implantable medical devices (Khatoon et al., 2018; Gnanadhas et al., 2015), biofouling of industrial systems (Characklis et al., 1981; Di Gregorio et al., 2017), product contamination (Niboucha et al., 2022), corrosion (Garret et al., 2008), and system failures (NASA, 2019; Weir et al., 2012). Biofilm remediation provides a unique challenge, due to their well-documented tolerant nature (Bowler et al., 2020; Stewart, 2015). Biocides and antibiotics that target biofilm are necessary to decrease the rate of infection and contamination (Meade, 2021). There are multiple American Society for Testing and Materials (ASTM) standard test methods that may be followed to grow a reproducible biofilm including: ASTM E2562-22 (ASTM International, 2022), ASTM E3161-21 (ASTM International, 2021), ASTM E2647-20 (ASTM International, 2020), and ASTM E2196-23 (ASTM International, 2023). ASTM Method E2799-22 (ASTM International, 2022; Parker et al., 2014) describes how to both grow a biofilm and determine the efficacy of biocides against a mature biofilm. Standard test methods allow for consistency across the field (Wade et al., 2023), which is why regulators and industry use standard methods for informed decision making. Standard test methods are different from research methods in that every step of the process is clearly defined and approved by a consensus standard setting organization such as ASTM, International Organization for Standardization (ISO), Japanese Industrial Standards (JIS) and Association of Official Analytical Chemists (AOAC). More importantly, standard test methods level the playing field across diverse industries and provide confidence that the product does indeed achieve the label claim when used correctly.

The CDC Biofilm Reactor is a laboratory reactor system that has been used extensively to grow biofilms in moderate to high fluid shear following ASTM E2562-22 (Johnson et al., 2021) or ASTM E3161-21. The Single Tube Method, as described in ASTM E2871-21 (ASTM International, 2021), uses the biofilm grown in the CDC Biofilm Reactor for biocide efficacy testing. For companies to make a "kills biofilm" hospital level label claim, the US Environmental Protection Agency (U.S. EPA) requires use of the CDC Biofilm Reactor and the Single Tube Method to attain a minimum six log reduction in viable biofilm bacteria in each of 3 tests using *Pseudomonas aeruginosa* (ATCC 15442) and *Staphylococcus aureus* (ATCC 6538) (U.S. EPA, 2023)

Regulatory agencies rely on standard test methods for decision making because the statistical attributes of repeatability, reproducibility, ruggedness, and responsiveness have been validated, which enables regulators to set product performance standards based on the statistical attributes (Tomasino et al., 2014). The CDC Biofilm Reactor has excellent experiment-to-experiment repeatability (Goeres et al., 2005) and laboratory-to-laboratory reproducibility (Goeres et al., 2019). While repeatability and reproducibility of the biofilm grown in the CDC Biofilm Reactor has been demonstrated, there have not been any reports in the literature confirming that biofilms grow uniformly on the coupons at different heights and orientations in the reactor. Previous work has shown little difference in the average sheer environment of coupons at different depths (Johnson et al., 2021). Johnson et al. noted that the top coupons experience a slightly narrower distribution stress across their surface compared to the middle and bottom coupons. However, the baffle side and glass side of the coupons experience different shear forces. This is due to the baffled stir bar. The side of the coupon that faces the baffle is referred to throughout this paper as the baffle side of the coupon. The side of the coupons that

face the exterior glass beaker is referred to as the glass side throughout. The baffle side of the coupons experience more shear forces than the glass side of the coupons. This led us to hypothesize that there would be a higher log density on the glass side of the coupons.

In the United States, all hospital level disinfectants that want to add a kills biofilm claim are tested using the CDC Biofilm Reactor (CDC biofilm reactor - BioSurface Technologies Corporation, 2024) as described in ASTM E3161-21 (ASTM International, 2022). Therefore, it is important to determine if position of the coupons within the reactors affects biofilm density. This ensures that products are evaluated using the most unbiased approach and regulatory decisions affirm the safety and efficacy of products.

This paper addresses the question as to whether coupon selection would bias results due to different growth on the coupon surface depending on its height within the reactor and orientation towards the glass or baffle. The experiments reported here were used to determine if the colony forming unit (CFU) measure of biofilm growth on the coupons at different heights and orientations were statistically equivalent.

Methods

Biofilm Growth

The CDC Biofilm Reactor (CDC Biofilm Reactor - BioSurface Technologies Corporation, 2024) was used to grow *P. aeruginosa* (ATCC 15442) and *S. aureus* (ATCC 6538) biofilms according to ASTM E2562-22 (ASTM International, 2023) and ASTM E3161-21 (ASTM International, 2022) respectively.

Experimental design

A picture of the CDC Biofilm Reactor is shown in Figure 1. The log densities of the coupons at various heights and orientations were compared. Three runs of the experiment were executed over the course of three weeks each for *P. aeruginosa* and *S. aureus.* In each experiment, four rods were randomly sampled from the reactor. The baffle side of the top, middle, and bottom coupons were sampled from two of the rods and the glass side from two different rods, Figure 2. Whether the coupon was oriented towards the glass or baffle will hereafter be referred to as its orientation. This comparison created six different environments for the coupons: top-baffle, middle-baffle, bottom-baffle, top-glass, middle-glass, and bottom-glass.

Figure 1. The CDC Biofilm Reactor, pump, and 20-L carboy with nutrient broth (Single Tube Method Video, accessed on 11/15/2023).

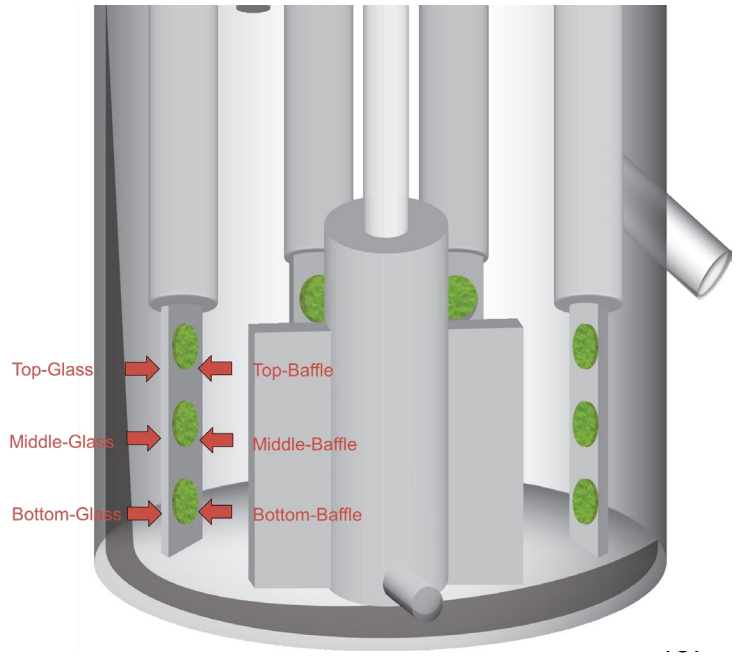

Figure 2. Orientation of coupons in the CDC Biofilm Reactor, identifying which coupons are referred to as top, middle, bottom and glass and baffle.

For each of the six experiments, *P. aeruginosa* ATCC 15442 and *S. aureus* ATCC 6538 were grown and inoculated according to the ASTM E3161 - 20 (ASTM International, 2022). The reactor was assembled and operated according to the ASTM E2562 - 22 (ASTM International, 2023).

Harvesting and enumeration of the biofilm

After 24 hours of continuous flow per ASTM E3161-18 (ASTM International, 2022), the pump was turned off and rods were randomly selected from the reactor to be sampled. The glass-side of the top, middle, and bottom coupons in two rods and the baffle-side of the top, middle, and bottom coupons from two different rods were sampled. The indicated surface was scraped into 9 mL of diluent, then 1mL of the diluent was pipetted over the scraped side of the coupon to

remove any remaining loosely adhered cells. The biofilm was disaggregated using a combination of sonication and vortexing, or homogenization. Sonication and vortexing was used in the first experiment with *P. aeruginosa*. The samples were vortexed for 30 seconds followed by 30 seconds of sonication. All twelve samples were vortexed three times and sonicated twice. Homogenization [IKA T25 Basic Homogenizer] was used for the second and third *P. aeruginosa* experiment and all three experiments using *S. aureus*. After homogenizing, the samples were serially diluted and plated on R2A agar plates for *P. aeruginosa* and tryptic soy agar (TSA) for *S. aureus* and incubated for 20 +/- 2 hours at 36 ℃. Colonies were counted and the CFU/cm^2 calculated.

Coupon image acquisition and analysis

Microscopic imaging was performed on an upright Leica TCS-SP5 Confocal Scanning Laser Microscope using the 488 and 561 nm laser excitation lines. Biofilms were stained with LIVE/DEAD *Bac*Light Bacterial Viability Kit stain (Thermo Fisher Scientific #L7012) for 20 minutes, rinsed, and then imaged in a fully-hydrated state using extra-long working distance water immersion objectives. The images were processed using Imaris x64 9.2.0 software (Bitplane Scientific Software, Zurich, Switzerland).

Statistical methods

The CFU/cm^2 for each side of the coupon were calculated according to ASTM E2871-21, then transformed to log densities and fit by a linear mixed effects model with a random effect for experiment and fixed effects for orientation, height, and the two-way interaction. Tukeys 90% confidence intervals were used to test for equivalence of the mean log densities at a 95% confidence level using an equivalency margin of 0.5 log (Richter and Richter, 2002). In other words, the absolute values of the lower confidence limits (LCL) and upper confidence limits

(UCL) had to be less than 0.5 to conclude equivalence. Minitab v21 was used for all statistical analyses and to create graphs.

Results

The purpose of the experiments was to determine whether the orientation and height of the coupons in the CDC Biofilm Reactor affected the biofilm cell density on the coupons of *P. aeruginosa* and *S. aureus* biofilm grown in independent experiments.

Pseudomonas aeruginosa

To determine the positional effects on biofilm density in the CDC reactor, *P. aeruginosa* biofilms were grown per ASTM E3161 (ASTM International, 2022). After the continuous flow phase, biofilm was scraped from the indicated surfaces to preserve positional data and prevent contributions from the biofilm on the opposite side. Figure 3 shows the $\log_{10}$ densities for *P. aeruginosa* across 3 independent experiments. The overall mean for all positions was 8.23 $\log_{10}$ CFU/cm^2. The mean biofilm density for each position ranged from 8.19 to 8.27 $\log_{10}$ CFU/cm^2. No trends were observed when comparing baffle side or vertical position. It was determined that *P. aeruginosa* densities were statistically equivalent amongst all coupon heights and orientations (Supplemental Materials, Table A.1). On the first *P. aeruginosa* run, sonication and vortexing were used instead of homogenization. However, there is no evidence that suggests there is a systematic difference when using sonication and vortexing instead of a homogenizer ($p = 0.232$).

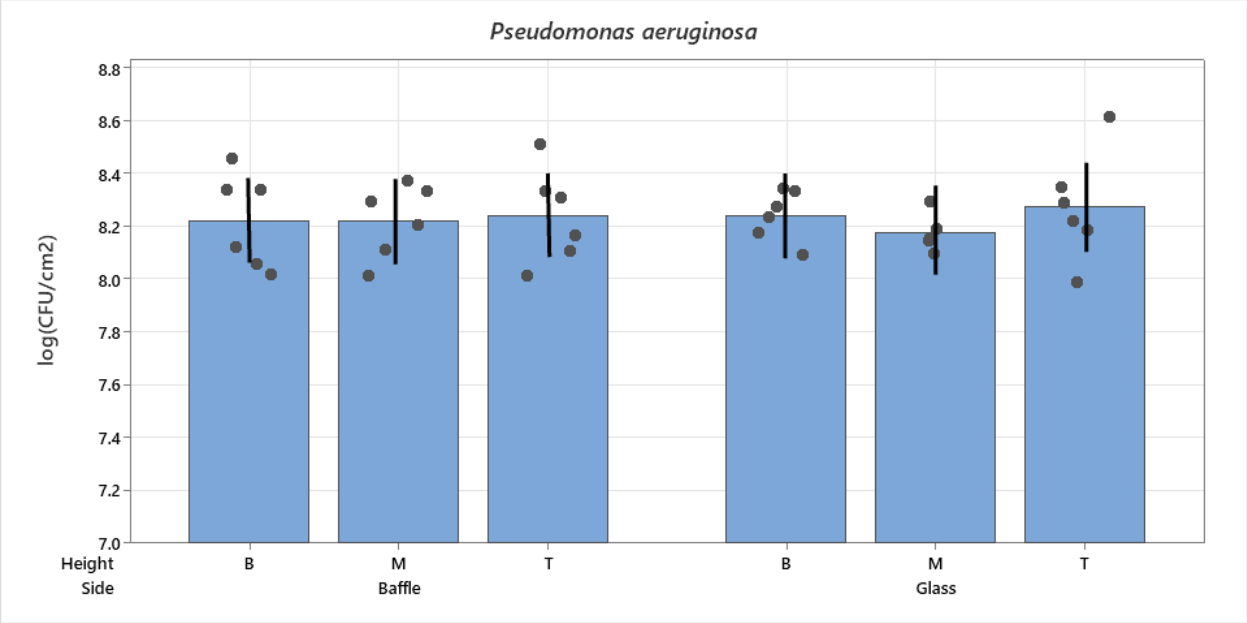

Figure 3. Coupon log densities across the three experimental runs comparing the baffle side bottom, middle, and top to the glass side bottom, middle, and top for *P. aeruginosa.* Individual points indicate the log density for a single coupon, tops of the bars indicate the mean, error bars indicate 90% confidence level.

Staphylococcus aureus

To determine the positional effects on biofilm density in the CDC reactor, *S. aureus* biofilms were grown per ASTM E3161 (ASTM International, 2022). After the continuous flow phase, biofilm was scraped from the indicated surfaces to preserve positional data and prevent contributions from the biofilm on the opposite side. Figure 4 shows the $\log_{10}$ densities for *S. aureus* across 3 independent experiments. The overall mean for all positions was 8.10 $\log_{10}$ CFU/cm^2. The mean biofilm density for each position ranged from 7.93 to 8.21 $\log_{10}$ CFU/cm^2. No trends were observed when comparing side or vertical position. Although *S. aureus* biofilm densities showed no differences ($p = 0.290$), the densities were not statistically equivalent among all coupon heights and orientations due to the variability in the data. There was greater variation

on the baffle-oriented coupons compared to the glass-oriented coupons (Supplemental Material, C.1).

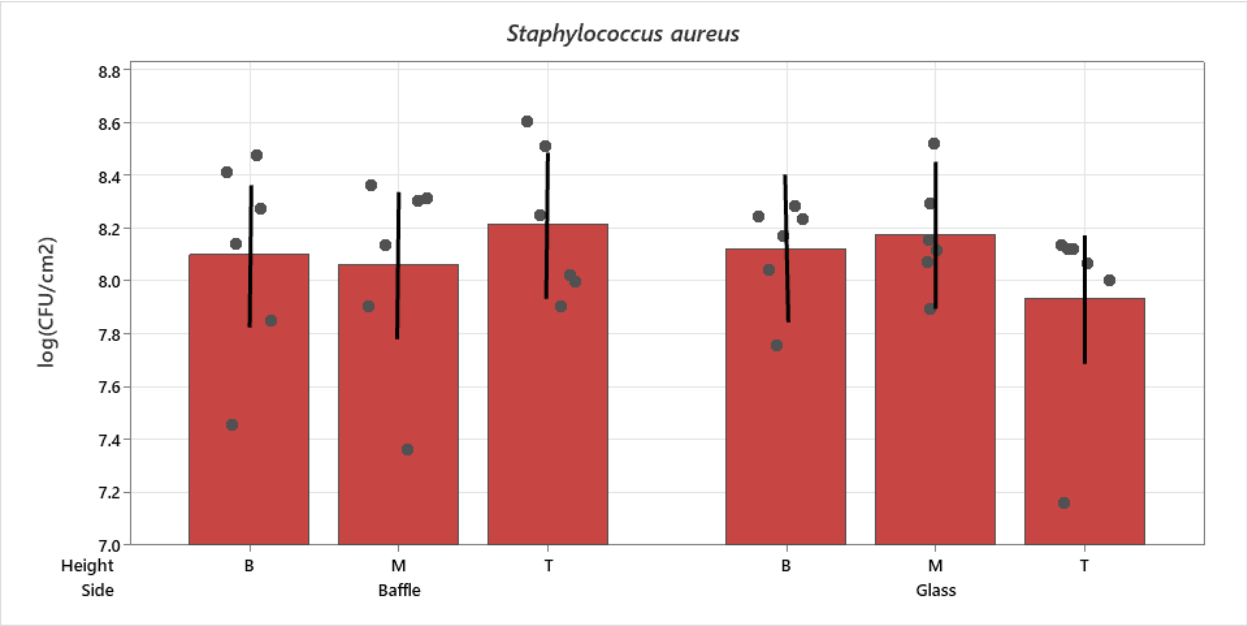

Figure 4. Coupon log densities across the three experimental runs comparing the baffle side bottom, middle, and top to the glass side bottom, middle, and top for *S. aureus.* Individual points indicate the log density for a single coupon, tops of the bars indicate the mean, error bars indicate 90% confidence level.

Imaging comparison

The *P. aeruginosa* viable cell counts demonstrated equivalence on the glass and baffle facing surfaces despite known differences in flow characteristics and resulting shear force. Confocal microscopy was used to assess if the differences in shear affected biofilm architecture and structure, Figure 5. The baffle orientation showed a highly structured, thick biofilm with a rough surface and numerous pronounced “mushroom” structures reminiscent of flow cell

biofilms subject to shear force. In contrast, the glass biofilm was thinner, with a more consistent structure and less roughness.

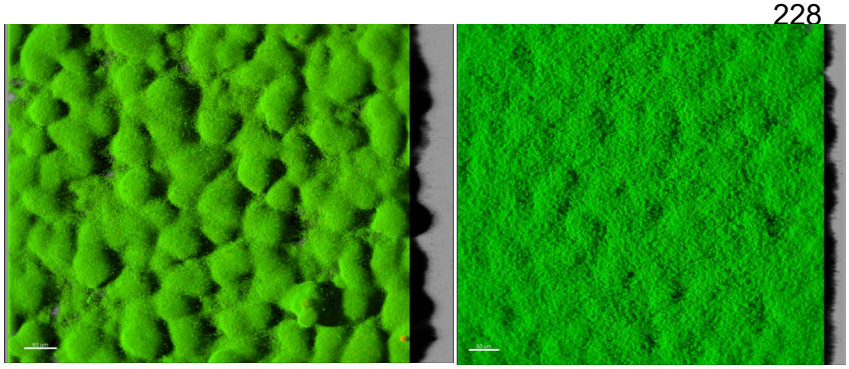

Figure 5. The morphological differences of a *P. aeruginosa* biofilm between the baffle-side (left image) and glass-side (right image) as captured by the upright Leica TCS-SP5 Laser Scanning Confocal Microscope. The images were taken with 250X magnification, scale bars represent 50µm.

Discussion

In the US, hospital level disinfectants with kills biofilm label claims have been evaluated using ASTM E3161-21 and E2871-21, however, no existing literature addresses if coupon orientation within the CDC biofilm reactor affects antimicrobial performance evaluations. Due to the importance of these regulatory decisions, it is essential to assess the equivalence or dissimilarities of the biofilms across positions in the CDC reactor.

This research suggests that when using the CDC Biofilm Reactor, the placement of the coupons in the reactor will not affect the viable cell log density. Nonetheless, a randomized design was recommended to select which coupons are used for control and treated samples. Randomized selection is required if there are differences in biofilm density between coupons at

different heights within the reactor and an orientation towards the glass or baffle. Showing statistical equivalence means that differences between the treatment coupons and control coupons are due solely to the treatment and not to the potential confounding effect of coupon height and orientation. Using an equivalency margin of 0.5 means that differences up to half a log are considered negligible and of no practical importance. This value has been used standard setting organizations (ASTM International E1054-22, 2022) and regulatory agencies (Nelson et al., 2013; Federal Register, 2017). Since the greatest difference between coupons was 0.32 log for *P. aeruginosa,* there is statistical equivalence across coupon height and orientation (Supplemental Material, Table A.1). Statistical equivalence for coupon orientation is important when the biofilm is harvested from the coupon using scraping, which uses one side of the coupon instead of sampling the biofilm from both sides. For *S. aureus* the absolute values for the LCL and UCL were greater than 0.5, therefore, there was no statistical equivalence between the coupon height and orientation (Supplemental Material, Table B.1).

Interestingly, even though the log density was equivalent for *P. aeruginosa* across all coupon height and orientation combinations, there are obvious visual differences between the baffle-side and glass-side of the coupons, Figure 5. The visual differences suggest that if a quantification method other than CFUs was used to analyze the biofilm growth, it may reflect differences between the baffle-side and glass-side of the coupon or even between the coupons at different heights. While the data showed increased variability on the baffle side compared to the glass side (Supplemental Material, Table D.1), there was still statistical equivalence among all six conditions for *P. aeruginosa*. It is important to note that for antimicrobial evaluations, the entire coupon is exposed to the test chemistry, so the results reported are an average of all surfaces. This study utilized scraping to isolate specific surfaces, which differs from the

established protocol in ASTM E2871-21 (ASTM International, 2021). While this study did not assess differences in biofilm susceptibility to antimicrobials between the structured baffle side biofilms and the smooth glass side biofilms, the mushroom structures are associated with differential motility (Barken et al., 2008) and expression of polysaccharides comprising the biofilm matrix (Jennings et al., 2015; Jones et al., 2013). Fleming noted that the localization of eDNA in *P. aeruginosa* formed a grid-like structure and a mushroom-like appearance. This study also mentioned that rhamnolipids found in the *P. aeruginosa* EPS matrix contribute to the formation of the mushroom-like structure (Flemming et al., 2010). What causes the structural formation of the matrix is an active area of study (Liu et al., 2022). Additionally, the strength of biofilm attachment is affected by many characteristics including fluid dynamics within the reactor, bacterial second messenger c-di-GMP (Alotaibi and Bukhari, 2021), and intercellular signaling systems (Johnson et al., 2021). It was noted that biofilm thickness is a key variable in biofilm structure and function (Suarez et al., 2019). Future work should assess if these structural difference affect biocide efficacy.

One reason that the CDC Biofilm Reactor is used regularly is that, like other standardized methods, repeatability and reproducibility of biofilm growth have been assessed and shown to be excellent (Goeres et al. 2019). A second reason is that it allows for 24 distinct sampling coupons so that various treatments can be tested at the same time. There are several variations of the CDC Biofilm Reactor, one of which was used to study the growth of *S. aureus* on polyetheretherketone (PEEK) membranes (Williams et al., 2011). The study showed that there was repeatability so the PEEK membranes can be used to inoculate animal model orthopedic implant biofilm-related infection. Another variation was modified to be able to grow biofilm on collagen (Miller et al., 2020). A limitation of the CDC Biofilm Reactor and the Single Tube

Method is that the efficacy is only quantified using viable plate counts. The matrix, biofilm architecture, proteins, or carbohydrates are not considered. Consequently, while the measure of efficacy determines if the bacteria are killed due to the application of a biocide, it does not consider if the matrix remains adhered to the surface. In terms of biofilm remediation, considering the strength of biofilm attachment, which is in part determined by the surface on which the biofilm is growing, is important when deciding upon biofilm removal strategies. The nature of the surface influences the cell attachment and viability and then the biofilm formation (Gedas et al., 2023). Surface attachment is also dependent on the bacteria present and the type of extracellular polymeric substances (EPS). The EPS mediates cell-cell and cell-surface adhesive interactions. Also, the concentration, cohesion, charge, and sorption capacity of the EPS will affect the biofilm's formation and maintenance (Flemming et al., 2010). The important role the biofilm matrix plays in growth and attachment suggests that assessing removal should be done using a matrix specific quantitative method, moving beyond the reliance on the viable plate count.

The crystal violet method has been used to evaluate the matrix following biocide treatment, and there are more selective probes that have been developed (Wilson et al., 2017; Kamimura et al., 2022). Wang et al sought to develop a method of measuring bacterial adhesion. They accomplished this with the use of a recombinant bioluminescent *P. aeruginosa* containing a lux reporter (Wang et al., 2021). They demonstrated that the bioluminescent method gave similar results to the viable plate count but with less potential variation due to human error (Wang et al., 2021). While the CFU counting method is still a very useful tool, further research on the matrix and architecture needs to be done to assess its impact on biofilm removal.

Conclusion

P. aeruginosa densities were statistically equivalent among all coupon heights and orientations, as long as differences of 0.32 logs are negligible and of no practical importance. *S. aureus* cell growth showed no statistically significant differences ($p = 0.290$). However, the densities were not statistically equivalent among all coupon heights and orientations due to the variability in the data. There was greater variation on the baffle-oriented coupons compared to the glass-oriented coupons. The results showed that no matter which coupons are sampled in the CDC Biofilm Reactor, it will not introduce bias into the results for *P. aeruginosa.* This research contributed additional information in the validation and standardization of biofilm growth methods using the CDC Biofilm Reactor. Finally, while this study demonstrated the accuracy and usefulness of the CDC Biofilm Reactor in growing biofilm and that the viable plate count method continues to provide valuable information about biofilm growth, additional methods should be considered for use alongside the viable plate count.

CrediT authorship contribution statement

EB: Conceptualization, Data curation, Formal analysis, Methodology, Roles/Writing – original draft; **KBM**: Methodology, Supervision, Writing – review & editing; **LM**: Visualization, Methodology, Supervision, Writing – review & editing; **AEP**: Conceptualization, Formal Analysis, Supervision, Writing – review & editing; **CJ:** Conceptualization, Writing – review & editing; **DMG**: Conceptualization, Project Administration, Resources, Supervision, Writing – review & editing.

Declaration of competing interest

The authors declare no conflicts of interest.

Data availability

Data will be made available on request.

References

[1] Alotaibi, G. F., & Bukhari, M. A. (2021, May 21). Factors influencing bacterial biofilm formation and development. *Biomedgrid.* DOI: 10.34297/AJBSR.2021.12.001820

[2] ASTM E1054-22, "Standard practices for evaluation of inactivators of antimicrobial agents" (ASTM International, 2022) DOI: 10.1520/E1054-21E01.

[3] ASTM E2196-23, "Standard test method for quantification of *Pseudomonas aeruginosa* biofilm grown with medium shear and continuous flow using rotating disk reactor" (ASTM International, 2023) DOI: 10.1520/E2196-23.

[4] ASTM E2871-21, "Standard test method for determining disinfectant efficacy against biofilm grown in the CDC Biofilm Reactor using the Single Tube Method" (ASTM International, 2020) DOI: 10.1520/E2871-21

[5] ASTM E2562-22, "Standard test method for quantification of *Pseudomonas aeruginosa* biofilm grown with high shear and continuous flow using CDC Biofilm Reactor" (ASTM International, 2023) DOI: 10.1520/E2562-22.

[6] ASTM E2647-20, "Standard test method for quantification of *Pseudomonas aeruginosa* biofilm grown using Drip Flow Biofilm Reactor with low shear and continuous flow" (ASTM International, 2020) DOI: 10.1520/E2647-20.

[7] ASTM E2799-22, "Standard test method for testing disinfectant efficacy against *Pseudomonas aeruginosa* biofilm using the MBEC Assay" (ASTM International, 2022) DOI: 10.1520/E2799–22.

[8] ASTM E3161-21, "A standard practice for preparing a *Pseudomonas aeruginosa* or *Staphylococcus aureus* biofilm using the CDC Biofilm Reactor" (ASTM International, 2022) DOI: 10.1520/E3161-21

[9] Barken, K. B., Pamp, S. J., Yang, L., Gjermansen, M., Bertrand, J. J., Klausen, M., Givskov, M., Whitchurch, C. B., Engel, J. N., & Tolker-Nielsen, T. (2008). Roles of type IV pili, flagellum-mediated motility and extracellular DNA in the formation of mature multicellular structures in *pseudomonas aeruginosa* biofilms. *Environmental Microbiology*, *10*(9), 2331–2343. DOI:10.1111/j.1462-2920.2008.01658.x https://enviromicro-journals.onlinelibrary.wiley.com/doi/epdf/10.1111/j.1462-2920.2008.01658.x?saml_referrer

[10] Bjarnsholt, T. (2013). The role of bacterial biofilms in chronic infections. *APMIS*, 121(s136), 1–58.https://doi.org/10.1111/apm.12099

[11] Bowler P, Murphy C, Wolcott R. Biofilm exacerbates antibiotic resistance: Is this a current oversight in antimicrobial stewardship? *Antimicrob Resist Infect Control.* 2020 Oct 20;9(1):162. DOI: 10.1186/s13756-020-00830-6. PMID: 33081846; PMCID: PMC7576703 https://www.ncbi.nlm.nih.gov/pmc/articles/PMC7576703/

[12] CDC biofilm reactor - Biosurface Technologies Corporation. BioSurface Technologies - Biofilm Reactors and Flow Cells. (2024, January 11). https://biofilms.biz/products/biofilm-reactors/cdc-biofilm-reactor/?gad_source=1&gclid=EAIaIQobChMIhc2185DlgwMVJcvCBB12-gzGEAAYASACEgL7EvD_BwE

[13] Characklis, W.G., Nevimons, M.J., & Picologlou, B.F. (1981). Influence of fouling biofilms on heat transfer. *Heat Transfer Engineering*, *3*(1), 23–37. https://doi.org/10.1080/01457638108939572

[14] Di Gregorio, L., Tandoi, V., Congestri, R., Rossetti, S., & Di Pippo, F. (2017). Unraveling the core microbiome of biofilms in Cooling Tower Systems. *Biofouling*, *33*(10), 793–806. https://doi.org/10.1080/08927014.2017.1367386

[15] Efficacy Test Methods, Test Criteria, and Labeling Guidance for Antimicrobial Products with Claims Against Biofilm on Hard, Non-Porous Surfaces (2023). In EPA.gov. Retrieved February 27, 2024 from https://www.epa.gov/pesticide-analytical-methods/efficacy-test-methods-test-criteria-and-labeling-guidance

[16] Federal Register, "Safety and Effectiveness of Health Care Antiseptics; Topical Antimicrobial Drug Products for Over-the-Counter Human Use, A Rule by the Food and Drug Administration, Fed. Reg. 82(243): 60487, 21 CFR 310, December 20, 2017, URL: https://www.federalregister.gov/documents/2017/12/20/2017-27317/safety-and-effectiveness-of-health-care-antiseptics-topical-antimicrobial-drug-products-for

[17] Flemming, H. C., & Wingender, J. (2010). The biofilm matrix. *Nature Reviews Microbiology,* 8(9), 623–633. https://doi.org/10.1038/nrmicro2415

[18] Garrett, T. R., Bhakoo, M., & Zhang, Z. (2008). Bacterial adhesion and biofilms on surfaces. *Progress in Natural Science*, 18(9), 1049–1056. https://doi.org/10.1016/j.pnsc.2008.04.001

[19] Gędas A., Draszanowska A., den Bakker H., Diez-Gonzalez F., Simões M., Olszewska M.A., (2023). Prevention of surface colonization and anti-biofilm effect of selected phytochemicals against listeria innocua strain. *Colloids and surfaces*, DOI: 10.1016/j.colsurfb.2023.113391 https://pubmed.ncbi.nlm.nih.gov/37290199/

[20] Goeres D.M., Loetterle L, Hamilton M.A. et al (2005). Statistical assessment of a laboratory method for growing biofilms. *Microbiology*, 151:757–762 DOI: 10.1099/mic.0.27709-0 https://pubmed.ncbi.nlm.nih.gov/15758222/

[21] Goeres, D. M., Walker, D. K., Buckingham-Meyer, K., Lorenz, L., Summers, J., Fritz, B., Goveia, D., Dickerman, G., Schultz, J., & Parker, A. E. (2019). Development, standardization, and validation of a biofilm efficacy test: The single tube method. *Journal of Microbiological Methods*, *165*, 105694. https://doi.org/10.1016/J.MIMET.2019.105694

[22] Gnanadhas, D. P., Elango, M., Janardhanraj, S., Srinandan, C. S., Datey, A., Strugnell, R. A., Gopalan, J., & Chakravortty, D. (2015). Successful treatment of biofilm infections using shock waves combined with antibiotic therapy. *Scientific Reports*, 5(1). https://doi.org/10.1038/srep17440

[23] Jennings, L. K., Storek, K. M., Ledvina, H. E., Coulon, C., Marmot, L. S., Sadovskaya, I., Secor, P. R., Tseng, B. S., Scian, M., Filloux, A., Wozniak, D. J., Howell, P. L., & Parsek, M. R. (2015). Pel is a cationic exopolysaccharide that cross-links extracellular DNA in the *Pseudomonas aeruginosa* biofilm matrix. *Proceedings of the National Academy of Sciences*, *112*(36), 11353–11358. https://doi.org/10.1073/pnas.1503058112

[24] Johnson, E., Petersen, T., & Goeres, D. M. (2021). Characterizing the shearing stresses within the CDC biofilm reactor using computational fluid dynamics. *Microorganisms*, 9(8), 1709. https://doi.org/10.3390/microorganisms9081709

[25] Jones, C. J., Ryder, C. R., Mann, E. E., & Wozniak, D. J. (2013). AMRZ modulates *Pseudomonas aeruginosa* biofilm architecture by directly repressing transcription of the *psl* operon. *Journal of Bacteriology*, *195*(8), 1637–1644. https://doi.org/10.1128/jb.02190-12

[26] Kamimura, R., Kanematsu, H., Ogawa, A., Kogo, T., Miura, H., Kawai, R., Hirai, N., Kato, T., Yoshitake, M., & Barry, D. M. (2022). Quantitative analyses of biofilm by using crystal violet staining and optical reflection. *Materials*, *15*(19), 6727. https://doi.org/10.3390/ma15196727

[27] Khatoon, Z., McTiernan, C. D., Suuronen, E. J., Mah, T.-F., & Alarcon, E. I. (2018, December 28). Bacterial biofilm formation on implantable devices and approaches to its treatment and prevention. *Heliyon*. DOI: 10.1016/j.heliyon.2018.e01067 https://www.ncbi.nlm.nih.gov/pmc/articles/PMC6312881/

[28] Liu, X.-Y., Guo, S., Bocklitz, T., Rösch, P., Popp, J., & Yu, H.-Q. (2022). Nondestructive 3D imaging and quantification of hydrated biofilm matrix by confocal Raman microscopy coupled with non-negative matrix factorization. *Water Research*, *210*, 117973. https://doi.org/10.1016/j.watres.2021.117973

[29] Meade, E., Slattery, M. A., & Garvey, M. (2021). Biocidal resistance in clinically relevant microbial species: A major public health risk. *Pathogens*, *10*(5), 598. https://doi.org/10.3390/pathogens10050598

[30] Miller, M., Rogers, J. C., Badham, M. A., Cadenas, L., Brightwell, E., Adams, J., Tyler, C., Sebahar, P. R., Haussener, T. J., Reddy, H. R., Looper, R. E., & Williams, D. L. (2020). Examination of a first-in-class bis-dialkylnorspermidine-terphenyl antibiotic in topical formulation against mono and polymicrobial biofilms. *PLOS ONE*, *15*(10). https://doi.org/10.1371/journal.pone.0234832

[31] NASA. (2019). Microbiological characterization of the International Space Station Water Processor Assembly External Filter Assembly S/N 01 - *NASA Technical Reports Server (NTRS)*. NASA. https://ntrs.nasa.gov/citations/20120015342

[32] Nelson, M. T., LaBudde, R. A., Tomasino, S. F., Pines, R. M., Bennett, M., Dormstetter, K., Eastman, T., Hellickson, L., Hollingsworth, A., Juhnke, A., Klein, D., Mitchell, J., Otte, M., Pines, R., Schwarz, S., & Tomasino, S. (2013). Comparison of 3MTM Petrifilm™ aerobic count plates to standard plating methodology for use with AOAC antimicrobial efficacy methods 955.14, 955.15, 964.02, and 966.04 as an alternative enumeration procedure: Collaborative Study. *Journal of AOAC INTERNATIONAL*, *96*(4), 717–722. https://doi.org/10.5740/jaoacint.12-469

[33] Niboucha, N., Goetz, C., Sanschagrin, L., Fontenille, J., Fliss, I., Labrie, S., & Jean, J. (2022, May 23). Comparative study of different sampling methods of biofilm formed on stainless-steel surfaces in a CDC biofilm reactor. *Frontiers.* https://doi.org/10.3389/fmicb.2022.892181

[34] Parker, A. E., Walker, D. K., Goeres, D. M., Allan, N., Olson, M. E., & Omar, A. (2014). Ruggedness and reproducibility of the MBEC biofilm disinfectant efficacy test. *Journal of Microbiological Methods*, 102, 55–64. https://doi.org/10.1016/j.mimet.2014.04.013

[35] Richter, S. J., & Richter, C. (2002). A method for determining equivalence in industrial applications. *Quality Engineering*, *14*(3), 375–380. https://doi.org/10.1081/qen-120001876

[36] Stewart P.S. (2015). Antimicrobial Tolerance in Biofilms. *Microbiol Spectr.* 3(3). DOI: 10.1128/microbiolspec.MB-0010-2014. https://doi.org/10.1128/microbiolspec.mb-0010-2014

[37] Suarez, C., Piculell, M., Modin, O., Langenheder, S., Persson, F., & Hermansson, M. (2019). Thickness determines microbial community structure and function in nitrifying biofilms via deterministic assembly. *Nature News*. https://doi.org/10.1038/s41598-019-41542-1

[38] Tomasino, S. F., Parker, A. E., & Hamilton, M. A. (2014). Use of statistical modeling to reassess the performance standard for the AOAC use-dilution methods (955.15 and 964.02). *Journal of AOAC International*, 97(1), 68-77. DOI: https://doi.org/10.5740/jaoacint.13-216

[39] Wade, S. A., Webb, J. S., Eckert, R. B., Jenneman, G. E., Rice, S. A., Skovhus, T. L., Sturman, P., Kotu, S. P., Richardson, M., & Goeres, D. M. (2023). The role of standards in biofilm research and Industry Innovation. *International Biodeterioration & Biodegradation*, 177, 105532. https://doi.org/10.1016/j.ibiod.2022.105532

[40] Wang, L., Qiao, X., Gao, L., Chen, C., & Wan, Y. (2021, February 28). A quantitative method to assess bacterial adhesion using recombinant bioluminescent *Pseudomonas aeruginosa*. *Biophysics reports*. DOI: 10.52601/bpr.2021.200043 https://www.ncbi.nlm.nih.gov/pmc/articles/PMC10240536/

[41] Weir, N., Wilson, M., Yoets, A., Molina, T., Bruce, R., & Carter, L. (2012, July). Microbiological Characterization of the International Space Station Water Processor Assembly External Filter Assembly S/N 01. In 42nd International Conference on Environmental Systems (p. 3595) https://ntrs.nasa.gov/citations/20120015342

[42] Williams, D. L., Woodbury, K. L., Haymond, B. S., Parker, A. E., & Bloebaum, R. D. (2011). A modified CDC biofilm reactor to produce mature biofilms on the surface of peak membranes for an in vivo animal model application. *Current Microbiology*, *62*(6), 1657–1663. https://doi.org/10.1007/s00284-011-9908-2

[43] Wilson, C., Lukowicz, R., Merchant, S., Valquier-Flynn, H., Caballero, J., Sandoval, J., Okuom, M., Huber, C., Brooks, T. D., Wilson, E., Clement, B., Wentworth, C. D., & Holmes, A. E. (2017). Quantitative and qualitative assessment methods for biofilm growth: A Mini-review. *Research & reviews. Journal of engineering and technology*. https://www.ncbi.nlm.nih.gov/pmc/articles/PMC6133255/

[44] YouTube. (2018, August 20). *Single Tube Method Video*. YouTube. https://www.youtube.com/watch?v=vwpxkOqYkhU&t=17s

Supplemental Material

Table A.1 shows the simultaneous 90% confidence intervals rounded to two decimals for the height x side comparison and the difference of means for *P. aeruginosa.*

Difference of Height*Side Levels	Difference of Means	Simultaneous 90% CI
(B Glass) - (B Baffle)	0.0203	(-0.21, 0.25)
(M Baffle) - (B Baffle)	0.0003	(-0.22, 0.22)
(M Glass) - (B Baffle)	-0.0320	(-0.28, 0.21)
(T Baffle) - (B Baffle)	0.0185	(-0.21, 0.24)
(T Glass) - (B Baffle)	0.0520	(-0.18, 0.28)
(M Baffle) - (B Glass)	-0.0200	(-0.25, 0.21)
(M Glass) - (B Glass)	-0.0523	(-0.29, 0.19)
(T Baffle) - (B Glass)	-0.0018	(-0.23, 0.23)
(T Glass) - (B Glass)	0.0317	(-0.19, 0.26)
(M Glass) - (M Baffle)	-0.0323	(-0.28, 0.21)
(T Baffle) - (M Baffle)	0.0183	(-0.21, 0.24)
(T Glass) - (M Baffle)	0.0518	(-0.18, 0.28)
(T Baffle) - (M Glass)	0.0505	(-0.19, 0.29)
(T Glass) - (M Glass)	0.0840	(-0.15, 0.32)
(T Glass) - (T Baffle)	0.0335	(-0.20, 0.26)

Table B.1 shows the simultaneous 90% confidence intervals for the height x side comparison and the difference of means for *S. aureus.*

Difference of Height*Side Levels	Difference of Means	Simultaneous 90% CI
(B Glass) - (B Baffle)	0.021	(-0.48, 0.52
(M Baffle) - (B Baffle)	-0.038	(-0.53, 0.46)
(M Glass) - (B Baffle)	0.075	(-0.42, 0.57)
(T Baffle) - (B Baffle)	0.115	(-0.38, 0.61)
(T Glass) - (B Baffle)	-0.167	(-0.66, 0.33)
(M Baffle) - (B Glass)	-0.059	(-0.55, 0.44)
(M Glass) - (B Glass)	0.054	(-0.44, 0.55)
(T Baffle) - (B Glass)	0.094	(-0.40, 0.59)
(T Glass) - (B Glass)	-0.187	(-0.68, 0.31)
(M Glass) - (M Baffle)	0.113	(-0.38, 0.61)
(T Baffle) - (M Baffle)	0.153	(-0.34, 0.65)
(T Glass) - (M Baffle)	-0.128	(-0.62, 0.37)
(T Baffle) - (M Glass)	0.040	(-0.46, 0.54)
(T Glass) - (M Glass)	-0.241	(-0.74, 0.25)
(T Glass) - (T Baffle)	-0.281	(-0.78, 0.21)

Table C.1 shows the standard deviations for all six conditions for *Staphylococcus aureus.*

Height/Side	Standard Deviation
Bottom/Baffle	8.10 +/- 0.387
Middle/Baffle	8.06 +/- 0.383
Top/Baffle	8.21 +/- 0.290
Bottom/Glass	8.12 +/- 0.1985
Middle/Glass	8.17 +/- 0.2135
Top/Glass	7.93 +/- 0.381

Table D.1 shows the standard deviations for all six conditions for *Pseudomonas aeruginosa.*

Height/Side	Standard Deviation
Bottom/Baffle	8.22 +/- 0.1786
Middle/Baffle	8.22 +/- 0.1393
Top/Baffle	8.24 +/- 0.1798
Bottom/Glass	8.24 +/- 0.0971
Middle/Glass	8.19 +/- 0.0730
Top/Glass	8.27 +/- 0.2070